European Journal of Radiology Open 10 (2023) 100480

Contents lists available at ScienceDirect

European Journal of Radiology Open

journal homepage: www.elsevier.com/locate/ejro

Original article

Value of pre-treatment ^{18}F-FDG PET/CT radiomics in predicting the prognosis of stage III-IV colorectal cancer

Na Wang [a,b], Meng Dai [a,b], Yan Zhao [c], Zhaoqi Zhang [a,b], Jianfang Wang [a,b], Jingmian Zhang [a,b], Yingchen Wang [a], Yunuan Liu [a], Fenglian Jing [a], Xinming Zhao [a,b,*]

[a] Department of Nuclear Medicine, The Fourth Hospital of Hebei Medical University, Shijiazhuang, Hebei 050011, China
[b] Hebei Provincial Key Laboratory of Tumor Microenvironment and Drug Resistance, Shijiazhuang 050011, China
[c] Department of Oncology, The Fourth Hospital of Hebei Medical University, Shijiazhuang 050011, China

ARTICLE INFO

Keywords:
Radiomics
Prognostic
Stage III-IV
Colorectal cancer
^{18}F-FDG
PET/CT

ABSTRACT

Background and purpose: To investigate the value of radiomics features extracted from pre-treatment ^{18}F-FDG PET/CT in predicting the outcomes of stage III-IV colorectal cancer (CRC), which may assist in clinical management strategies and precise treatment of stage III-IV CRC.

Materials and methods: 124 patients with pathologically confirmed stage III-IV CRC who underwent pre-treatment ^{18}F-FDG PET/CT scans were enrolled in this study. The least absolute shrinkage and selection operator Cox regression (LASSO-Cox) was used to select radiomics features, and the radiomics scores (Rad-scores) were calculated to build radiomics models. The performance of radiomics models was represented by the concordance index (C-index) and compared with clinical models and complex model. The bootstrap resampling method was used to create validation sets. Additionally, nomograms were developed based on complex models.

Results: The C-indices of the radiomics model for predicting PFS and OS were 0.712 (95%CI: 0.680–0.744) and 0.758 (0.728–0.789), respectively. In the clinical model, these values were 0.690 (0.664–0.0.717) and 0.738 (0.709–0.767), respectively. However, in the complex model were 0.734 (0.705–0.762) and 0.780 (0.754–0.807), respectively. The Kaplan–Meier curves demonstrated that the radiomics model could effectively separate patients with stage III-IV stage CRC into high- and low-risk groups ($p < 0.001$). Multivariate Cox regression analysis confirmed the independent prognostic value of Rad-scores.

Conclusion: Pre-treatment ^{18}F-FDG PET/CT radiomics features can stratify the risk of patients with stage III-IV CRC and accurately predict their outcomes. These findings could be clinically valuable for precision treatment and management decisions in stage III-IV CRC.

1. Introduction

Colorectal cancer (CRC) has become the third most common cancer and the second most common cause of cancer-related deaths worldwide [1]. Approximately 60% of patients with CRC have already locally advanced disease or experience distant metastases at the time of diagnosis, and their 5-year survival rate is relatively low [2]. Although targeted agents combined with chemotherapy regimens used for the treatment of metastatic CRC have significantly improved survival, the prognosis of patients with CRC remains an important factor in clinical patient management and selection of treatment decisions [3]. Therefore, the choice of treatment options and accurate assessments are crucial for predicting patients with III-IV stage CRC prognosis and individual treatment strategy decisions.

The tumor-node-metastasis (TNM) staging classification system plays an important role in predicting patients with III-IV CRC prognosis [4]. Tumor heterogeneity in pre-treatment ^{18}F-FDG PET/CT images may contribute to better characterization and improved prediction of malignant tumor survival outcomes[5]. Recently, radiomics has become the primary trend in medical imaging studies and has shown significant potential for the analysis of lesion characterization and intratumoral heterogeneity (ITH) [6,7]. It can extract large numbers of quantitative multidimensional and subvisual image features and excavate a large amount of image information to evaluate the biological characteristics

* Correspondence to: Department of Nuclear Medicine, The Fourth Hospital of Hebei Medical University, 12 Jiankang Road, Shijiazhuang, Hebei 050011, China.
E-mail address: xinm_zhao@163.com (X. Zhao).

https://doi.org/10.1016/j.ejro.2023.100480
Received 31 October 2022; Received in revised form 30 January 2023; Accepted 4 February 2023

of tumors [8–10] . Radiomics studies for CRC prognosis are mostly based on computed tomography (CT) or magnetic resonance imaging (MRI) [11–14]. However, there are few reports on the prediction of stage III-IV CRC using ^{18}F-fluorodeoxyglucose positron emission tomography/-computed tomography (^{18}F-FDG PET/CT) radiomics. Thus, this study aimed to develop and validate a baseline ^{18}F-FDG PET/CT radiomics model to predict patients with stage III-IV CRC outcomes; the findings may have a potential application value in clinical management strategies and precise treatment of stage III-IV CRC.

2. Materials and methods

2.1. Patient selection

This retrospective, single-institution study was approved by the institutional ethics committee (approval no. 2021KY292), which waived the requirement for informed consent from patients. A database of 124 patients with stage III-IV CRC who underwent pre-treatment ^{18}F-FDG PET/CT screening between February 2014 and September 2020 in our department was assessed.

The inclusion criteria were as follows: (1) primary lesions of stage III-IV CRC pathologically confirmed as adenocarcinoma, (2) ^{18}F-FDG PET/CT examination within 1 month of pathological examination and 2 weeks before initial treatment, (3) no history of other malignant tumors, (4) complete clinical data, and (5) no loss to follow-up. The exclusion criteria were as follows: (1) patients with stage I-II CRC, (2) antitumor therapy before ^{18}F-FDG PET/CT screening, (3) double or multiple primary CRC, (4) pathological diagnosis not obtained from the primary CRC lesions, and (5) tumor metabolic volume on PET/CT images < 5 cm^3.

Of the 124 patients with CRC enrolled based on the above criteria, 82 were male and 42 were female, with an average age of 58.69 $\pm$ 12.16 (range, 26–83) years. Moreover, 36 and 88 patients were diagnosed with CRC in the colon and rectum, respectively. The patient screening process is shown in Fig. 1.

2.2. Positron emission tomography/computed tomography imaging and acquisition parameters

Each patient underwent ^{18}F-FDG PET/CT examination using GEMINI GXL PET/CT (PHILIPS) scanner equipped with a 16-slice CT 1 month before treatment. After fasting 6 h, ^{18}F-FDG was injected intravenously with 3.7–5.5 MBq/kg (0.1–0.15 mCi/kg). Blood glucose level was maintained at 11 mmol/L. Whole-body PET/CT examination was performed 60 min after ^{18}F-FDG injection.

According to the Image Biomarker Standardization Initiative reporting guidelines [15], the scan parameters are shown in Table S1.

2.3. Segmentation and radiomics feature extraction

PET/CT images of all patients in the Digital Imaging and Communications in Medicine format were successively imported to the Local Image Features Extraction (LIFEx) package (version 7.0.0, http://www.lifexsoft.org) [16]. Two experienced nuclear medicine physicians independently used 40% of the maximum standardized uptake value (SUVmax) [17] as an optimization threshold to delineate the region of interest (ROI) of the CRC primary lesions using the LIFEx package. Manual segmentation was performed along the contour of the tumor during delineation to avoid the inclusion of intestinal gas, fatty tissue around the intestinal wall, and surrounding cords into the scope of the ROI. When it was difficult to determine the boundary of lesions, the boundary was determined by adjusting the window width and position or by combining coronal and sagittal images. The spatial resampling intervals X, Y, and Z on the PET/CT images were 2 mm $\times$ 2 mm $\times$ 2 mm for all patients [16,18]. Absolute intensity resampling setting are as follows: absolute value range: CT images were set as $-$ 1000–3000HU, PET image were set as 0–25SUV. Intensity discretization setting: CT images were set as 0–400bins, PET images were set as 0–64bins.

2.4. Radiomics feature selection and model building

First, we standardized the radiomics features extracted from ^{18}F-FDG

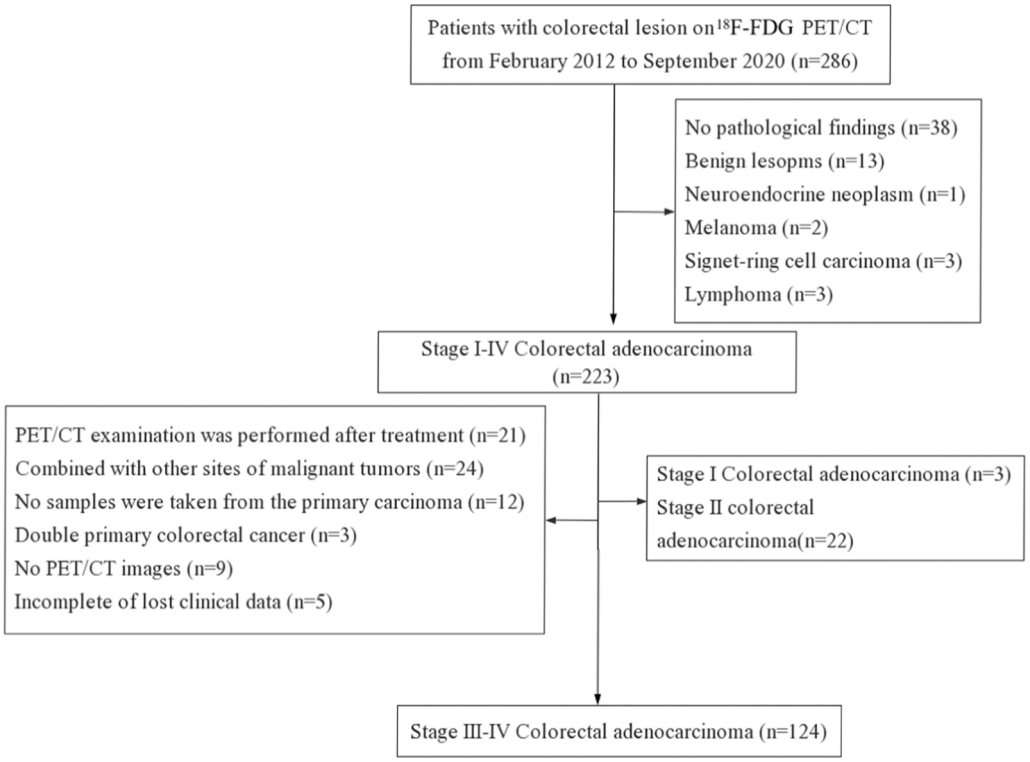

Fig. 1. The flowchart shows the process of selection.

PET/CT. Then, the PET/CT radiomics features predicting progression-free survival (PFS) and overall survival (OS) were screened using least absolute shrinkage and selection operator Cox regression (LASSO-Cox), and linear fitting was conducted according to their respective coefficient weights [17]. Cross-validation was applied to select radiomics features with nonzero coefficients. The radiomics score (Rad-score) of each patient was calculated using the formula used to construct the radiomics models. We determined the optimal threshold of the Rad-score on the Youden index of the receiver operating characteristic curve and divided patients into high- and low-risk groups based on the optimal threshold of the Rad-score. Kaplan–Meier (K–M) analysis and log-rank test were used to evaluate the potential association between the radiomics model and PFS and OS.

Univariate and multivariate Cox regression analyses were performed to select significant clinical variables that predicted the prognosis of PFS and OS in stage III-IV CRC to build a clinical model. The Rad-score and significant clinical variables were entered into a multivariate Cox regression to construct the complex model.

2.5. Model validation

The Harrell concordance index (C-index) was used to evaluate the performance of the three models [19,20]. Bootstrap resampling 1000 times was used to obtain the corrected C-index of the three models for internal verification. Based on the best prediction model, a nomogram was developed that could intuitively and effectively predict the risk probability of each patient. In addition, the accuracy and repeatability of the model were visually evaluated using the Hosmer–Lemeshow test and calibration curves, and the deviation from the theoretical perfect calibration was not significant ($p > 0.05$) [21].

2.6. Follow-up of patients

All patients were followed every 3–6 months after treatment during the first 2 years and every 6 months thereafter. In this study, PFS was defined as the time from the date of pathological diagnosis of CRC to the follow-up confirmation of tumor progression, death, or follow-up cutoff. OS was defined as the time from the date of pathological diagnosis of CRC to the confirmation of death or the cut-off date of follow-up. The follow-up period ended on September 30, 2021.

2.7. Statistical analyses

Statistical analyses were performed using the International Business Machines Statistical Package for the Social Sciences Statistics version 26.0 and R 4.2.1 software packages (http://www.R-project.org). The C-index values of radiomic model, clinical model and complex model were compared by compareC software in R language. All results were considered statistically significant at $p < 0.05$.

3. Results

3.1. Follow-up patients

The median follow-up times of PFS and OS were 20.5 and 28.6 (range, 1.1–60.5) months, respectively. Of the 124 patients, 70 (56.45%) experienced relapse, and 61 (49.19%) died during the follow-up period. At the follow-up date, the PFS rates at 1, 2, and 3 years were 62.10%, 50.55%, and 39.52%, respectively, and the OS rates were 83.06%, 66.93%, and 53.23%, respectively.

3.2. Clinical characteristics of patients and Cox analysis of prognostic factors

The basic clinical characteristics of the enrolled patients and the univariate and multivariate Cox regression analyses for predicting PFS and OS are summarized in Tables 1 and 2, respectively. For PFS, Tumor location ($p = 0.009$), Tumor diameter ($p = 0.042$), Lymphatic metastasis ($p < 0.001$), Distant metastasis ($p < 0.001$), Therapy method ($p < 0.001$), and carbohydrate antigen 199 (CA199) level ($p = 0.012$) were statistically significant in the univariate Cox regression analysis. However, multivariate Cox analysis showed that only Distant metastasis ($p < 0.001$) was an independent prognostic factor for PFS. The Tumor location ($p < 0.001$), Distant metastasis ($p < 0.001$), Lymphatic metastasis ($p < 0.001$), Distant metastasis ($p < 0.001$), Therapy method ($p < 0.001$), and CA199 level ($p = 0.024$) were prognostic factors for OS in univariate Cox regression analysis. But only Distant metastasis ($p < 0.001$) and Therapy method ($p = 0.013$) were independent prognostic factors for OS in multivariate Cox regression analysis.

3.3. Radiomics features analysis and model establishment

A total of 196 PET/CT radiomics features (98 PET and 98 CT features) were extracted (Table S2). According to the LASSO-Cox results (Fig. 2), Eleven and twelve PET/CT radiomics features with nonzero coefficients for predicting PFS and OS were obtained, respectively, to construct radiomics models.

For PFS, the screened 11 PET/CT radiomic features include 3 PET and 8 CT imaging features. The three PET radiomic features were as follows: Conventional_SUVKurtosis, Discretized_SUVKurtosis, Grey-Level Size Zone Matrix_Small Zone Low Grey Emphasis (GLZLM_SZLGE), the eight CT radiomic features were Conventional_HUKurtosis, Discretized_HUmax, Discretized_HUQ2, Discretized_HUQ3, SHAPE_Compacity, Grey-Level Co-occurrence Matrix_Homogeneity (GLCM_Homogeneity), Grey-Level Run Length Mrtrix_Short Run Gray-Level Emphasis (GLRLM_SRHGE), Grey-Level Size Zone Matrix_Small Zone High Gray Emphasis (GLZLM_SZHGE). The Rad_score of each patient for predicting PFS was calculated using the following formula.

$$Rad\_scorePFS = -0.125 \times Conventional\_SUVKurtosis - 0.292 \times Discretized\_SUVKurtosis - 0.159 \times GLZLM\_SZLGE - 0.014 \times Conventional\_HUKurtosis + 0.359 \times Discretized\_HUmax - 0.112 \times Discretized\_HUQ2 - 0.084 \times Discretized\_HUQ3 - 0.129 \times SHAPE\_Compacity + 0.184 \times GLCM\_Homogeneity - 0.284 \times GLRLM\_SRHGE + 0.031 \times GLZLM\_SZHGE$$

The selected 12 radiomics features which including five PET and seven CT radiomic features for predicting OS were: Conventional_SUVKurtosis, Discretized_SUVKurtosis, Discretized_HISTO_Energy, GLZLM_SZLGE, Grey-Level Size Zone Matrix_Zone Percentage (GLZLM_ZP) (PET radiomic features), Conventional_HUKurtosis, Discretized_HUmax, Discretized_HUQ2, Discretized_HUQ3, SHAPE_Sphericity, SHAPE_Compacity, GLRLM_SRHGE (CT radiomic features). For OS, the Rad-score formula for each patient was as follows:

$$Rad\_socreOS = -0.090 \times Convent$$

Table 1
Baseline clinical characteristics of stage III-IV CRC patients, univariate and multivariate Cox regression analysis for predicting PFS in stage III-IV CRC patients.

Characteristics	All patients (N = 124)	Univariate analysis			Multivariate analysis		
		HR	95%CI	*P*-value	HR	95%CI	*P*-value
Gender, n (%)		1.29	0.80–2.09	0.292			
Male	82 (66.1%)						
Female	42 (33.9%)						
Age, n (%)		1.14	0.72–1.81	0.585			
< 61	61(49.2%)						
≥ 61	63(50.8%)						
Tumor location, n (%)		0.52	0.32–0.85	0.009*	1.29	0.76–2.20	0.341
Colon	36(29.0%)						
Rectum	88(71.0%)						
Tumor diameter, n (%)		0.62	0.38–0.98	0.042*	0.97	0.58–1.61	0.904
< 5.0 cm	61(49.2%)						
≥ 5.0 cm	63(50.8%)						
T stage, n (%)		1.24	0.77–2.01	0.384			
$T_{2–3}$	81(65.3%)						
T_4	43(34.7%)						
Lymphatic metastasis, n (%)		0.39	0.24–0.63	< 0.001*	1.18	0.65–2.14	0.596
No	32(25.8%)						
Yes	92(74.2%)						
Distant metastasis, n (%)		5.26	3.07–9.00	< 0.001*	4.36	2.44–7.81	< 0.001*
No	62(50.0%)						
Yes	62(50.0%)						
Therapy method, n (%)		2.81	1.75–4.53	< 0.001*	1.57	0.94–2.64	0.087
Comprehensive surgical treatment	69(55.6%)						
Nonoperative comprehensive treatment	55(44.4%)						
BMI, n (%)		0.79	0.49–1.27	0.327			
< 24.9	68(54.8%)						
≥ 24.9	56(45.2%)						
CEA, n (%)		1.27	0.73–2.18	0.398			
< 5 ng/mL	33(26.6%)						
≥ 5 ng/mL	91(73.4%)						
CA199, n (%)		1.82	1.14–2.89	0.012*	1.25	0.77–2.04	0.370
< 27.0 ng/mL	74(59.7%)						
≥ 27.0 ng/mL	50(40.3%)						
Rad_score	/	/	/	/	2.56	1.46–4.48	0.001*

BMI, body mass index; CEA, carcinoembryonic antigen; CA199, carbohydrate antigen199; / not apply. * $P < 0.05$.

$$\begin{aligned} &ional\_SUVKurtosis - 0.149 \times Discretized\_SUVKurtosis - 0.018 \\ &\times Discretized\_HISTO\_Energy - 0.026 \times GLZLM\_SZLGE + 0.090 \\ &\times GLZLM\_ZP - 0.006 \times Conventional\_HUKurtosis + 0.363 \\ &\times Discretized\_HUmax - 0.228 \times Discretized\_HUQ2 - 0.007 \\ &\times Discretized\_HUQ3 - 0.105 \times SHAPE\_Sphericity - 0.144 \\ &\times SHAPE\_Compacity - 0.650 \times GLRLM\_SRHGE \end{aligned}$$

Regardless of the radiomics model used for predicting PFS and OS, the Rad-score in the high- and low-risk groups was statistically significant ($p < 0.001$). Stage III-IV CRC Patients with high Rad-scores had poor survival outcomes.

3.4. Performance of the radiomics features, clinical variables, and complex model

The results of the C-index and Hosmer–Lemeshow test are shown in Table 3. The C-indices of the radiomics model for predicting PFS and OS were 0.712 (95% CI: 0.680–0.744) and 0.758 (0.728–0.789), respectively, which were 0.690 (0.664–0.717) and 0.738 (0.709–0.767), respectively, in the clinical model. However, the complex models based on Rad-score and clinical variables had higher C-indices (i.e., 0.734, 95% CI: 0.705–0.762, and 0.780, 95% CI: 0.754–0.807, respectively). The C-indices between complex model and radiomics model in predicting PFS and OS were statistically different (both $p < 0.001$). And there was a statistically significant difference in the C-index for predicting PFS and OS between the complex and the clinical model (PFS: $p = 0.003$; OS: $p = 0.011$). The findings were confirmed by bootstrap resampling (n = 1000).

3.5. Individualized nomogram construction and calibration curve

We divided the patients into high- and low-risk groups according to the optimum cutoff point of the Rad-score (Rad-score$_{PFS}$ = −0.0031, Rad-score$_{OS}$ = 0.0612). In the relapse risk stratification, 71 (57.5%) patients were classified into the high-risk group, and 58 (81.7%) of these patients experienced recurrence at the overall endpoint. A total of 53 (42.7%) patients were assigned to the low-risk group, of which 18 (34.0%) developed recurrence by the overall endpoint. The K–M curve demonstrated that the risk of recurrence was significantly higher in the high-risk group than in the low-risk group ($p < 0.001$) (Fig. 3A). For OS, 52 (41.9%) patients were in the high-risk group, and 42 (80.8%) had fatal events. In total, 72 (58.1%) patients were assigned to the low-risk group, and among them, 19 (26.4%) died. The K–M curve indicated that the risk of death in the high-risk group was significantly different from that in the low-risk group ($p < 0.001$) (Fig. 3B).

The median and interquad distances Conventional_SUVkurtosis PET radiomic feature to predict PFS into high- and low risk group were − 0.219 (−0.270, −0.154) and − 0.126 (−0.226, 0.031), respectively ($p < 0.001$). Discretized_SUVkurtosis has a median and interquartile interval of 0.245 (−0.303, −0.175) and 0.147 (−0.254, 0.124) in the high- and low-risk group, respectively ($p < 0.001$). The median and interquinqual intervals of Conventional_SUVkurtosis were − 0.215 (−0.269, −0.132) and − 0.180 (−0.251, −0.061), respectively to the predicted high- and low-risk groups ($p = 0.072$). Discretized_SUVkurtosis has a median and interquartile interval of − 0.244 (−0.302, −0.152) and − 0.192 (−0.277, −0.063), respectively, in the high-risk and low-risk groups for predicting deaths ($p = 0.035$).

Considering that the complex model based on independent predictive factors, including Rad-score and clinical variables (Distant

Table 2
Baseline clinical characteristics of stage III-IV CRC patients, univariate and multivariate Cox regression analysis for predicting OS in stage III-IV CRC patients.

Characteristics	All patients (N = 124)	Univariate analysis			Multivariate analysis		
		HR	95%CI	*P*-value	HR	95%CI	*P*-value
Gender, n (%)		1.42	0.85–2.38	0.182			
Male	82 (66.1%)						
Female	42 (33.9%)						
Age, n (%)		1.31	0.79–2.12	0.298			
< 61	61(49.2%)						
≥ 61	63(50.8%)						
Tumor location, n (%)		0.39	0.23–0.65	< 0.001*	0.92	0.50–1.69	0.786
Colon	36(29.0%)						
Rectum	88(71.0%)						
Tumor diameter, n (%)		0.63	0.38–1.05	0.074			
< 5.0 cm	61(49.2%)						
≥ 5.0 cm	63(50.8%)						
T stage, n (%)		1.39	0.83–2.34	0.215			
$T_{1–3}$	81(65.3%)						
T_4	43(34.7%)						
Lymphatic metastasis, n (%)		0.26	0.15–0.44	< 0.001*	0.77	0.42–1.41	0.389
No	32(25.8%)						
Yes	92(74.2%)						
Distant metastasis, n (%)		6.04	3.27–11.17	< 0.001*	4.88	2.55–9.34	< 0.001*
No	62(50.0%)						
Yes	62(50.0%)						
Therapy method, n (%)		3.25	1.93–5.49	< 0.001*	2.01	1.16–3.50	0.013*
Comprehensive surgical treatment	69(55.6%)						
Nonoperative comprehensive treatment	55(44.4%)						
BMI, n (%)		0.62	0.37–1.04	0.070			
< 24.9	68(54.8%)						
≥ 24.9	56(45.2%)						
CEA, n (%)		1.21	0.68–2.17	0.519			
< 5 ng/mL	33(26.6%)						
≥ 5 ng/mL	91(73.4%)						
CA199, n (%)		1.79	1.08–2.96	0.024*	1.18	0.70–1.98	0.542
< 27.0 ng/mL	74(59.7%)						
≥ 27.0 ng/mL	50(40.3%)						
Rad_score	/	/	/	/	2.90	1.65–5.11	< 0.001*

BMI, body mass index; CEA, carcinoembryonic antigen; CA199, carbohydrate antigen199; / not apply. * $P < 0.05$.

metastasis and Therapy method), had a better ability to predict PFS and OS, we developed a nomogram that could intuitively predict the risk proportion of each factor and individually predict the prognosis of patients (Fig. 4A, E). The calibration curves of the nomogram for predicting PFS and OS are shown in Fig. 4B–D and F–H and visually evaluated the consistency between the predicted and actual survival probabilities. The Hosmer–Lemeshow test was not statistically significant in either the complex model for predicting PFS ($\chi^2 = 0.150$, $p = 0.928$) or OS ($\chi^2 = 11.605$, $p = 0.071$).

4. Discussion

In this study, we developed and validated a baseline ^{18}F-FDG PET/CT radiomics model with moderate predictive ability for PFS and OS in patients with stage III-IV CRC. The radiomics signature is an independent risk factor for prognosis and provides a noninvasive method for stratifying the risk of recurrence or death in patients with stage III-IV CRC. Furthermore, complex models that combine Rad-score and optimal clinical variables to predict CRC outcomes were developed, and they showed significantly better predictive ability than a single radiomics or clinical model. The visualized nomogram based on complex models can identify patients at a high risk of early progression or death and provide individualized treatment strategies that are beneficial for these patients. The K–M curve indicated that our radiomics models could effectively distinguish between high- and low-risk groups in patients with stage III-IV CRC.

In this retrospective study, among the ^{18}F-FDG PET/CT radiomics features associated with PFS and OS, SUVkurtosis was a basic PET feature of the area under the curve of the cumulative SUV volume histogram. The SUVkurtosis was lower in the high-risk group than in the low-risk group. Compared with SUVmean, SUVkurtosis improves data fluctuation caused by statistical noise and is less susceptible to variations caused by subjective factors, and the data are more objective, to facilitate data comparison between different studies. Wagner et al. showed that the kurtosis of ^{18}F-FDG PET/CT parameters was significantly different between primary colon cancer lesions and hepatic metastases, which plays an important role in evaluating the heterogeneity of colon cancer [22]. Other studies have shown that the absolute gradient (GrKurtosis) is significantly associated with the 3-year disease-free survival (DFS) of locally advanced rectal cancer (LARC) and is an independent prognostic indicator of the outcome of LARC [23]. In our study, we found that patients with stage III-IV CRC with low SUVkurtosis had a higher risk of recurrence or death, which is consistent with the above findings.

The PET/CT first-order radiomics features that we screened to predict the prognosis in stage III-IV CRC also included Histogram based feature, Discretized_HISTO_Energy (PET feature), and two shape-based features, SHAPE_Compacity and SHAPE_Sphericity (CT features). The HISTO_Energy feature mainly describe the intensity of changes in the gray intensity information (or brightness information) of the lesions. In general, the smaller the change, the larger the HISTO_energy value. Some studies have shown that HISTO_Energy which extracted from ^{18}F-FDG PET/CT can predict disease-free survival (DFS) in patients with non-small cell lung cancer (NSCLC) [24] and OS in patients with esophageal cancer [25]. SHAPE_Compacity describes the degree of sphericity of the lesion, that is, it reflects the Compactness of the lesion. SHAPE_Sphericity is a feature that describes how similar an ROI is to a sphere, ideally with a sphericity of 1. Both are important factors for predicting the response of rectal cancer to nCRT [26,27], and have significant correlation with clinical prognostic factors [28]. Some

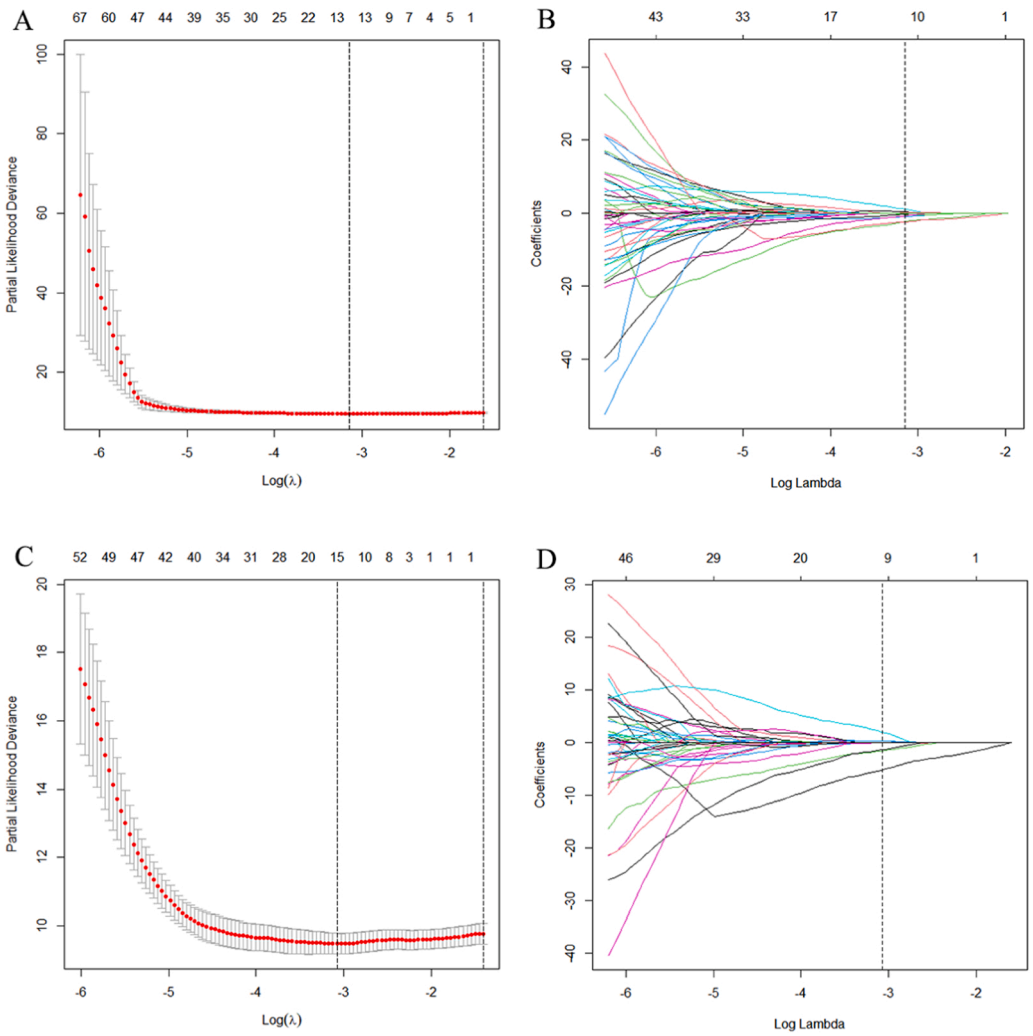

Fig. 2. The LASSO-Cox were used to select radiomic features to predicting PFS and OS. 10-fold cross-validation with the minimum criteria were used in the LASSO-Cox to select λ (A) PFS and 11 nonzero coefficients produced with the optimal λ (B) PFS. 10-fold cross-validation with the minimum criteria were used in the LASSO-Cox to select λ (C) OS and 12 nonzero coefficients produced with the optimal λ (D) OS.

Table 3
The results of the C-index and the Hosmer-Lemeshow.

	C-index (95CI %)	corected C-index (Bootstrap, B=1000)	χ^2 value	*p* value[a]
PFS				
Radiomics model	0.712 (0.680–0.744)	0.671 (0.723–0.834)	6.741	0.565
Clinical model	0.690 (0.664–0.717)	0.689 (0.639–0.744)	0.000	1.000
Complex model	0.734 (0.705–0.762)	0.730 (0.678–0.788)	0.150	0.928
OS				
Radiomics model	0.758 (0.728–0.789)	0.718 (0.682–0.795)	7.286	0.506
Clinical model	0.738 (0.709–0.767)	0.736 (0.680–0.794)	2.470	0.291
Complex model	0.780 (0.754–0.807)	0.772 (0.723–0.834)	11.605	0.071

χ^2 and [a]*p* value for the Hosmer-Lemeshow test.

studies reported that the three radiomics features showed good repeatability[26,29]. In our study, the three radiomics features could predict PFS or OS in patients with stage III-IV CRC.

Among the eleven and twelve ^{18}F-FDG PET/CT radiomics features associated with PFS and OS, there were four (one PET texture features GLZLM_SZLGE, and three CT texture feature, including GLCM_homogeneity, GLRLM_SRHGE and GLZLM_SZHGE) and three (two PET texture feature, including GLZLM_SZLGE and GLZLM_ZP, and one CT texture features GLRLM_SRHGE) second-order texture features, respectively. GLRLM, GLZLM, and GLCM are second-order texture parameters commonly used to quantify ITH. However, tumors with higher heterogeneity have poor prognosis [30]. In this study, patients with stage III-IV CRC with a high risk of recurrence or death had higher ITH. PET or multimodal imaging enables fine characterization of ITH in a noninvasive manner [31]. Previous studies have also shown that texture features based on GLCM, GLRLM, and GLZLM can capture spatial relations between adjacent pixels of a given image, which is a hot topic in radiomics and is closely related to prognosis [32]. Kang et al. established a prognostic prediction model for 381 patients with CRC using preoperative ^{18}F-FDG PET/CT radiomics features and found that GLRLM_LRE and GLZLM_SZLGE were independent factors of PFS [33]. Our study also showed that the texture features GLRLM and GLZLM were independent indicators of PFS and OS. The selected texture parameters differ among different studies, which may be attributed to the stability of texture features affected by imaging equipment, imaging technology, and reconstruction parameters.

Some scholars have attempted to predict the prognosis of patients with CRC using radiomics based on CT or MRI. Xue et al. found that the C-index of the nomogram, which was built by combining the Rad-score

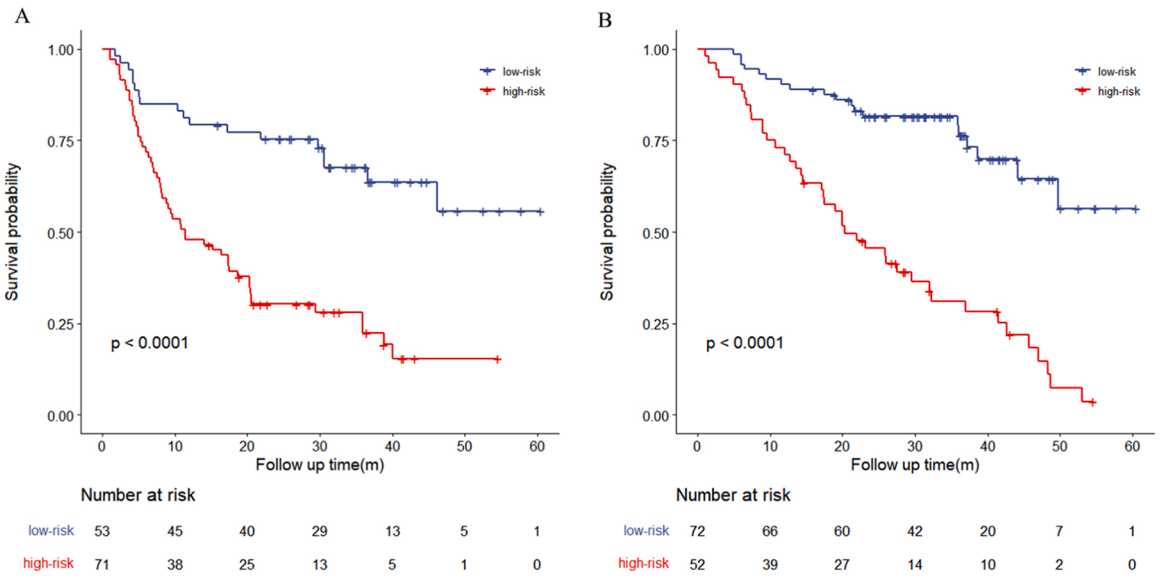

Fig. 3. The Kaplan-Meier survival analysis stratified the risk of recurrence or death based on the radiomics (A) PFS and (B) OS. The log-rank test was used to calculate *p* value.

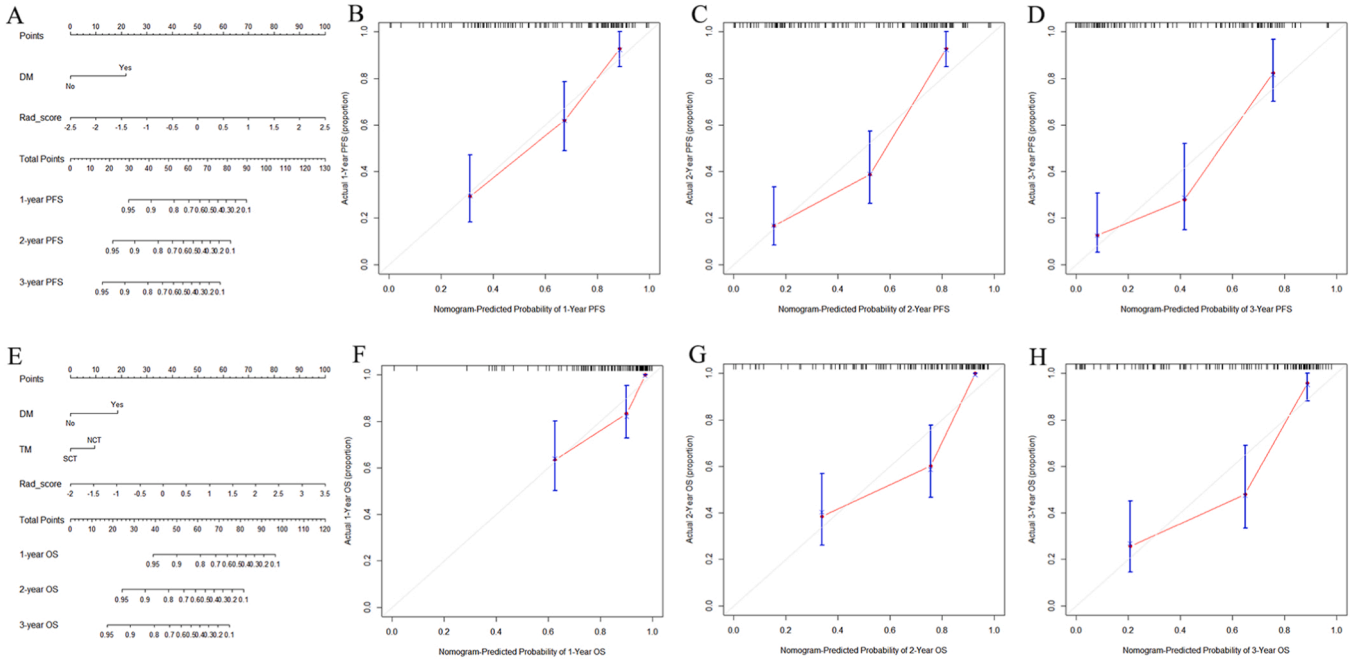

Fig. 4. The nomograms were developed combined Rad_score and clinical variables, A is for PFS and E is for OS. Calibration curves based on complex model for 1–3 year PFS (B-D) and OS (F-H).

with clinical factors to predict OS was 0.782, 0.721 and 0.677. These findings might affect treatment strategies of CRC [34]. Other scholars have developed a comprehensive model combining MRI radiomics features, morphological imaging models, and clinicopathological models to predict the 3-year OS of 206 patients with rectal cancer who underwent radical surgery, with a C-index of 0.872, which has a good predictive ability for OS [35]. However, there have been few studies on the application of imaging features extracted from PET/CT to predict the prognosis of CRC. Recently, a radiomics nomogram has been developed using ^{18}F-FDG PET/CT radiomics features, lymph node staging, and lymphovascular invasion and has shown good predictive power in patients with CRC, comparable to American Joint Committee on Cancer's staging systems in calibration. Their C-indices were 0.737 and 0.64, respectively, and the study demonstrated that ^{18}F-FDG PET/CT radiomics features may enable detailed stratification of outcomes in patients with CRC [33]. Another study used machine learning to develop and validate an integrated clinico-biological model based on ^{18}F-FDG PET/CT radiomics features had good predictive performance in predicting recurrence-free survival RFS in 196 patients with stage I–IV CRC. A previous study showed that ^{18}F-FDG PET/CT radiomics provides the possibility for precision treatment of CRC [36]. However, none of these studies demonstrated the predictive performance of a single^{18}F-FDG PET/CT radiomics model in predicting the outcomes of patients with CRC. In this study, we established pre-treatment ^{18}F-FDG PET/CT radiomics, clinical, and complex models to predict the outcomes of patients with stage III-IV CRC. The results demonstrated that the radiomics

model had good predictive ability in predicting PFS and OS, but the complex model showed the best predictive ability, which was consistent with the results of the above two studies. Therefore, our classifier was able to predict the prognosis and stratify the risk of patients with CRC.

Although ^{18}F-FDG PET/CT radimoic features can be applied to a variety of diseases, its application in colorectal cancer is increasing, and it has formed a relatively complete theoretical system and workflow, but it still faces some challenges. First, most of the current studies on ^{18}F-FDG PET/CT radiomic are single-center, small-sample retrospective studies, and large-sample, multi-center, randomized controlled prospective studies are needed for model validation, so as to verify the robustness and reproducibility of the model. Second, the potential relationship between some ^{18}F-FDG PET/CT radiomic features and tumor heterogeneity, such as anatomical, physiological or metabolic levels, is unknown and lack of explanation.

5. Conclusion

In conclusion, the establishment of a pre-treatment ^{18}F-FDG PET/CT radiomics model provides significant prognostic information about PFS and OS in patients with stage III-IV CRC and demonstrates important stratification power in predicting PFS and OS in CRC. Therefore, it may be helpful to guide precision treatment and clinical management decisions for patients with stage III-IV CRC.

Funding statement

This study was supported by the Senile disease Prevention and control Progject of Hebei Provincial Finance Department and Hebei Provincial Health Committee [grant number, 2020459]; the Key Project of Medical Science Research of Hebei Provincial Health Commission [grant number 20221345].

CRediT authorship contribution statement

Na Wang: Data curation, Formal analysis, Methodology, Project administration, Resources, Software, Validation, Writing – original draft. **Meng Dai:** Data curation, Methodology, Resources, Supervision, Validation, Writing – review & editing. **Yan Zhao:** Formal analysis, Methodology, Software, Visualization, Writing – review & editing. **Zhaoqi Zhang:** Data curation, Formal analysis, Supervision, Visualization, Writing – review & editing. **Jianfang Wang:** Formal analysis, Investigation, Supervision, Visualization. **Jingmian Zhang:** Investigation, Validation, Visualization, Writing – review & editing. **Yingchen Wang:** Data curation, Software, Validation. **Yunuan Liu:** Investigation, Software. **Fenglian Jing:** Methodology, Software. **Xinming Zhao:** Conceptualization, Formal analysis, Funding acquisition, Investigation, Project administration, Resources, Supervision, Writing – original draft.

Declaration of Competing Interest

The authors declare that they have no known competing financial interests or personal relationships that could have appeared to influence the work reported in this paper.

Acknowledgments

The authors thank all their participants involved in the study for their assistance and support.

Ethical statement

This retrospective, single-institution study was approved by the Ethics Committee of the Fourth Hospital of Hebei Medical University (approval no. 2021KY292), which waived the requirement for informed consent from patients. The patient data used in this study are confidential and anonymous.

Appendix A. Supporting information

Supplementary data associated with this article can be found in the online version at doi:10.1016/j.ejro.2023.100480.

References

[1] H. Sung, J. Ferlay, R.L. Siegel, M. Laversanne, I. Soerjomataram, A. Jemal, F. Bray, Global Cancer Statistics 2020: GLOBOCAN estimates of incidence and mortality worldwide for 36 cancers in 185 countries, CA Cancer J. Clin. 71 (2021) 209–249, https://doi.org/10.3322/caac.21660.

[2] R.L. Siegel, K.D. Miller, A. Goding Sauer, S.A. Fedewa, L.F. Butterly, J.C. Anderson, A. Cercek, R.A. Smith, A. Jemal, Colorectal cancer statistics, CA Cancer J. Clin. 70 (2020) 145–164, https://doi.org/10.3322/caac.21601.

[3] L.L. Gunderson, J.M. Jessup, D.J. Sargent, F.L. Greene, A. Stewart, Revised tumor and node categorization for rectal cancer based on surveillance, epidemiology, and end results and rectal pooled analysis outcomes, J. Clin. Oncol. 28 (2010) 256–263, https://doi.org/10.1200/JCO.2009.23.9194.

[4] G.J. Tong, G.Y. Zhang, J. Liu, Z.Z. Zheng, Y. Chen, P.P. Niu, X.T. Xu, Comparison of the eighth version of the American Joint Committee on Cancer manual to the seventh version for colorectal cancer: A retrospective review of our data, World J. Clin. Oncol. 9 (2018) 148–161, https://doi.org/10.5306/wjco.v9.i7.148.

[5] K.Y. Ko, C.J. Liu, C.L. Ko, R.F. Yen, Intratumoral Heterogeneity of Pretreatment 18F-FDG PET Images Predict Disease Progression in Patients With Nasal Type Extranodal Natural Killer/T-cell Lymphoma, Clin. Nucl. Med 41 (12) (2016) 922–926, https://doi.org/10.1097/RLU.0000000000001375.

[6] M.D. Kuo, N. Jamshidi, Behind the numbers: Decoding molecular phenotypes with radiogenomics–guiding principles and technical considerations, Radiology 270 (2014) 320–325, https://doi.org/10.1148/radiol.13132195.

[7] K. Bera, N. Braman, A. Gupta, V. Velcheti, A. Madabhushi, Predicting cancer outcomes with radiomics and artificial intelligence in radiology, Nat. Rev. Clin. Oncol. 19 (2022) 132–146, https://doi.org/10.1038/s41571-021-00560-7.

[8] Y.Q. Huang, C.H. Liang, L. He, J. Tian, C.S. Liang, X. Chen, Z.L. Ma, Z.Y. Liu, Development and validation of a radiomics nomogram for preoperative prediction of lymph node metastasis in colorectal cancer, J. Clin. Oncol. 34 (2016) 2157–2164, https://doi.org/10.1200/JCO.2015.65.9128.

[9] J.Y. Kim, J.E. Park, Y. Jo, W.H. Shim, S.J. Nam, J.H. Kim, R.E. Yoo, S.H. Choi, H. S. Kim, Incorporating diffusion- and perfusion-weighted MRI into a radiomics model improves diagnostic performance for pseudoprogression in glioblastoma patients, Neuro-Oncol. 21 (2019) 404–414, https://doi.org/10.1093/neuonc/noy133.

[10] P. Lovinfosse, M. Ferreira, N. Withofs, A. Jadoul, C. Derwael, A.N. Frix, J. Guiot, C. Bernard, A.N. Diep, A.F. Donneau, M. Lejeune, C. Bonnet, W. Vos, P.E. Meyer, R. Hustinx, Distinction of lymphoma from sarcoidosis at FDG PET/CT - evaluation of radiomic-feature guided machine learning versus human reader performance, J. Nucl. Med (2022), https://doi.org/10.2967/jnumed.121.263598.

[11] W. Dai, S. Mo, L. Han, W. Xiang, M. Li, R. Wang, T. Tong, G. Cai, Prognostic and predictive value of radiomics signatures in stage I-III colon cancer, Clin. Transl. Med 10 (2020) 288–293, https://doi.org/10.1002/ctm2.31.

[12] A. Dohan, B. Gallix, B. Guiu, K. Le Malicot, C. Reinhold, P. Soyer, J. Bennouna, F. Ghiringhelli, E. Barbier, V. Boige, J. Taieb, O. Bouché, E. François, J.M. Phelip, C. Borel, R. Faroux, J.F. Seitz, S. Jacquot, M. Ben Abdelghani, F. Khemissa-Akouz, D. Genet, J.L. Jouve, Y. Rinaldi, F. Desseigne, P. Texereau, E. Suc, C. Lepage, T. Aparicio, C. Hoeffel, Early evaluation using a radiomic signature of unresectable hepatic metastases to predict outcome in patients with colorectal cancer treated with FOLFIRI and bevacizumab, Gut 69 (2020) 531–539, https://doi.org/10.1136/gutjnl-2018-316407.

[13] Z. Liu, X. Meng, H. Zhang, Z. Li, J. Liu, K. Sun, Y. Meng, W. Dai, P. Xie, Y. Ding, M. Wang, G. Cai, J. Tian, Predicting distant metastasis and chemotherapy benefit in locally advanced rectal cancer, Nat. Commun. 11 (2020) 4308, https://doi.org/10.1038/s41467-020-18162-9.

[14] D. Daye, A. Tabari, H. Kim, K. Chang, S.C. Kamran, T.S. Hong, J. Kalpathy-Cramer, M.S. Gee, Quantitative tumor heterogeneity MRI profiling improves machine learning-based prognostication in patients with metastatic colon cancer, Eur. Radio. 31 (2021) 5759–5767, https://doi.org/10.1007/s00330-020-07673-0.

[15] A. Zwanenburg, M. Vallières, M.A. Abdalah, H. Aerts, V. Andrearczyk, A. Apte, S. Ashrafinia, S. Bakas, R.J. Beukinga, R. Boellaard, M. Bogowicz, L. Boldrini, I. Buvat, G. Cook, C. Davatzikos, A. Depeursinge, M.C. Desseroit, N. Dinapoli, C. V. Dinh, S. Echegaray, I. El Naqa, A.Y. Fedorov, R. Gatta, R.J. Gillies, V. Goh, M. Götz, M. Guckenberger, S.M. Ha, M. Hatt, F. Isensee, P. Lambin, S. Leger, R. Leijenaar, J. Lenkowicz, F. Lippert, A. Losnegård, K.H. Maier-Hein, O. Morin, H. Müller, S. Napel, C. Nioche, F. Orlhac, S. Pati, E. Pfaehler, A. Rahmim, A. Rao, J. Scherer, M.M. Siddique, N.M. Sijtsema, J. Socarras Fernandez, E. Spezi, R. Steenbakkers, S. Tanadini-Lang, D. Thorwarth, E. Troost, T. Upadhaya, V. Valentini, L.V. van Dijk, J. van Griethuysen, F. van Velden, P. Whybra, C. Richter, S. Löck, The image biomarker standardization initiative: standardized quantitative radiomics for high-throughput image-based phenotyping, Radiology 295 (2020) 328–338, https://doi.org/10.1148/radiol.2020191145.

[16] C. Nioche, F. Orlhac, S. Boughdad, S. Reuzé, J. Goya-Outi, C. Robert, C. Pellot-Barakat, M. Soussan, F. Frouin, I. Buvat, LIFEx: a freeware for radiomic feature calculation in multimodality imaging to accelerate advances in the

characterization of tumor heterogeneity, Cancer Res 78 (2018) 4786–4789, https://doi.org/10.1158/0008-5472.CAN-18-0125.
[17] H. Wang, S. Zhao, L. Li, R. Tian, Development and validation of an (18)F-FDG PET radiomic model for prognosis prediction in patients with nasal-type extranodal natural killer/T cell lymphoma, Eur. Radio. 30 (2020) 5578–5587, https://doi.org/10.1007/s00330-020-06943-1.
[18] Z. Du, X. Zhang, Z. Tang, More evidence for prediction model of radiosensitivity, Biosci. Rep. 41 (2021), https://doi.org/10.1042/BSR20210034.
[19] A. Weiss, M. Chavez-MacGregor, D.Y. Lichtensztajn, M. Yi, A. Tadros, G. N. Hortobagyi, S.H. Giordano, K.K. Hunt, E.A. Mittendorf, Validation Study of the American Joint Committee on Cancer Eighth Edition Prognostic Stage Compared With the Anatomic Stage in Breast Cancer, JAMA Oncol. 4 (2018) 203–209, https://doi.org/10.1001/jamaoncol.2017.4298.
[20] M. Amit, C. Liu, F.O. Netto Gleber, S. Kini, S. Tam, A. Benov, M. Aashiq, A.K. El-Naggar, A.C. Moreno, D.I. Rosenthal, B.S. Glisson, R. Ferrarotto, M.K. Wong, M. R. Migden, G. Li, A. Khanna, R.P. Goepfert, P. Nagarajan, R.S. Weber, J.N. Myers, N.D. Gross, Integrating depth of invasion in T classification improves the prognostic performance of the American Joint Committee on Cancer primary tumor staging system for cutaneous squamous cell carcinoma of the head and neck, Eur. J. Cancer (Oxf., Engl.: 1990) 144 (2021) 169–177, https://doi.org/10.1016/j.ejca.2020.11.019.
[21] M.J. Pencina, D.R.B. Sr, E.W. Steyerberg, Extensions of net reclassification improvement calculations to measure usefulness of new biomarkers, Stat. Med 30 (2011) 11–21, https://doi.org/10.1002/sim.4085.
[22] F. Wagner, Y.A. Hakami, G. Warnock, G. Fischer, M.W. Huellner, P. Veit-Haibach, Comparison of Contrast-Enhanced CT and [(18)F]FDG PET/CT Analysis Using Kurtosis and Skewness in Patients with Primary Colorectal Cancer, Mol. Imaging Biol. 19 (2017) 795–803, https://doi.org/10.1007/s11307-017-1066-x.
[23] J.I. Bang, S. Ha, S.B. Kang, K.W. Lee, H.S. Lee, J.S. Kim, H.K. Oh, H.Y. Lee, S. E. Kim, Prediction of neoadjuvant radiation chemotherapy response and survival using pretreatment [(18)F]FDG PET/CT scans in locally advanced rectal cancer, Eur. J. Nucl. Med. Mol. Imaging 43 (2016) 422–431, https://doi.org/10.1007/s00259-015-3180-9.
[24] M. Kirienko, F. Gallivanone, M. Sollini, G. Veronesi, E. Voulaz, L. Antunovic, L. Leonardi, G. Testanera, I. Castiglioni, A. Chiti, FDG PET/CT as theranostic imaging in diagnosis of non-small cell lung cancer, Front Biosci. (Landmark Ed.) 22 (2017) 1713–1723, https://doi.org/10.2741/4567.
[25] K.G. Foley, R.K. Hills, B. Berthon, C. Marshall, C. Parkinson, W.G. Lewis, T. Crosby, E. Spezi, S.A. Roberts, Development and validation of a prognostic model incorporating texture analysis derived from standardised segmentation of PET in patients with oesophageal cancer, Eur. Radio. 28 (2018) 428–436, https://doi.org/10.1007/s00330-017-4973-y.
[26] H. Park, K.A. Kim, J.H. Jung, J. Rhie, S.Y. Choi, MRI features and texture analysis for the early prediction of therapeutic response to neoadjuvant chemoradiotherapy and tumor recurrence of locally advanced rectal cancer, Eur. Radio. 30 (2020) 4201–4211, https://doi.org/10.1007/s00330-020-06835-4.
[27] N.P. Karahan Şen, A. Aksu, G.Ç. Kaya, Value of volumetric and textural analysis in predicting the treatment response in patients with locally advanced rectal cancer, Ann. Nucl. Med 34 (2020) 960–967, https://doi.org/10.1007/s12149-020-01527-x.
[28] A. Davey, M. van Herk, C. Faivre-Finn, H. Mistry, A. McWilliam, Is tumour sphericity an important prognostic factor in patients with lung cancer, Radio. Oncol. 143 (2020) 73–80, https://doi.org/10.1016/j.radonc.2019.08.003.
[29] M. Yan, W. Wang, A non-invasive method to diagnose lung adenocarcinoma, Front Oncol. 10 (2020) 602, https://doi.org/10.3389/fonc.2020.00602.
[30] R.J. Gillies, P.E. Kinahan, H. Hricak, Radiomics: images are more than pictures, they are data, Radiology 278 (2016) 563–577, https://doi.org/10.1148/radiol.2015151169.
[31] C. Bailly, C. Bodet-Milin, M. Bourgeois, S. Gouard, C. Ansquer, M. Barbaud, J. C. Sébille, M. Chérel, F. Kraeber-Bodéré, T. Carlier, Exploring Tumor Heterogeneity Using PET Imaging: The Big Picture, Cancers (Basel) 11 (2019), https://doi.org/10.3390/cancers11091282.
[32] G.L. Jensen, C.M. Yost, D.S. Mackin, D.V. Fried, S. Zhou, L.E. Court, D.R. Gomez, Prognostic value of combining a quantitative image feature from positron emission tomography with clinical factors in oligometastatic non-small cell lung cancer, Radio. Oncol. 126 (2018) 362–367, https://doi.org/10.1016/j.radonc.2017.11.006.
[33] J. Kang, J.H. Lee, H.S. Lee, E.S. Cho, E.J. Park, S.H. Baik, K.Y. Lee, C. Park, Y. Yeu, J.R. Clemenceau, S. Park, H. Xu, C. Hong, T.H. Hwang, Radiomics Features of 18F-Fluorodeoxyglucose Positron-Emission Tomography as a Novel Prognostic Signature in Colorectal Cancer, Cancers (Basel) 13 (2021), https://doi.org/10.3390/cancers13030392.
[34] T. Xue, H. Peng, Q. Chen, M. Li, S. Duan, F. Feng, A CT-based radiomics nomogram in predicting the postoperative prognosis of colorectal cancer: a two-center study, Acad. Radio. (2022), https://doi.org/10.1016/j.acra.2022.02.006.
[35] Z. Chuanji, W. Zheng, L. Shaolv, M. Linghou, L. Yixin, L. Xinhui, L. Ling, T. Yunjing, Z. Shilai, M. Shaozhou, Z. Boyang, Comparative study of radiomics, tumor morphology, and clinicopathological factors in predicting overall survival of patients with rectal cancer before surgery, Transl. Oncol. 18 (2022), 101352, https://doi.org/10.1016/j.tranon.2022.101352.
[36] L. Lv, B. Xin, Y. Hao, Z. Yang, J. Xu, L. Wang, X. Wang, S. Song, X. Guo, Radiomic analysis for predicting prognosis of colorectal cancer from preoperative (18)F-FDG PET/CT, J. Transl. Med 20 (2022) 66, https://doi.org/10.1186/s12967-022-03262-5.